RICHARD C. BENSON, C. BRENT BARGERON, NEWMAN deHAAS, R. BEN GIVENS, A. NORMAN JETTE, BERRY H. NALL, TERRY E. PHILLIPS, and FRANK G. SATKIEWICZ

SURFACE SCIENCE PROGRAM: RESEARCH AND APPLICATIONS TO APL PROBLEMS

Surface analytical techniques are reviewed, together with examples of their applications to several areas of interest at APL.

INTRODUCTION

The chemical and physical properties of surfaces and interfaces are important in many areas of interest at APL, including microelectronics, materials fabrication and processing, corrosion, adhesion, optical systems, spacecraft, and missile technology. Common to all of these general areas are basic phenomena such as adsorption, desorption, and surface chemical reactions, all of which are largely determined by surface composition and structure. Adsorption refers to the process that involves the adherence of an incident atom or molecule to a surface. This may be a physical process (physisorption) due to weak forces (van der Waals forces), or it may be chemical processes where strong bonds are formed between the surface and adsorbate (chemisorption). Adsorption should be distinguished from absorption since the latter consists of the penetration of a substance from one phase into the bulk (interior) of another by diffusion. Desorption is the process by which adsorbed species leave the surface.

The surface science program currently involves research in surface structure and surface/materials investigations using advanced analytical techniques. The latter area of effort is applied to microelectronic devices, spacecraft and missile materials, and specific failure analysis in collaboration with the Microelectronics Group and the Space, Aeronautics, and Fleet Systems Departments.

Surface atoms are in a different energy state than those in the bulk. An additional energy, known as surface energy, imparts to the surface unique physical and chemical properties that are largely dependent on the atomic arrangement of the surface. Our research on surface structure is motivated by the fact that knowledge of the atomic arrangements is essential in understanding surface phenomena, including electrical and optical properties and the manner in which chemical species adsorb and react. As examples, properties of the important Si/SiO_2 interface in silicon-based electronics are affected by the surface arrangement of silicon atoms, and epitaxial growth, which involves the fabrication of specially designed layers on prepared substrates, is critically dependent on the surface structure of the substrate.

Our work in surface/materials investigations in microelectronics arose a few years ago from a problem involving organic adhesives used in the fabrication of a hybrid microelectronic device for the Galileo spacecraft. Hybrid microelectronic devices consist of individual parts that are assembled into a single package. The substrate, typically a ceramic material with metallized conductive paths on the surface, is attached to the package. Next, discrete components (e.g., integrated circuits, individual semiconductor devices, resistors, and capacitors) are attached to the substrate. Wire bonds are then used to make electrical interconnections, and the package is subsequently hermetically sealed. The attachment of the substrate and components is done using either inorganic eutectics (such as gold-silicon) or organic adhesives (such as epoxies and polyimides). In the past, eutectics have been preferred because they do not contain organic chemicals that can lead more readily to reliability problems. However, as the size and number of individual components per hybrid have increased, organic adhesives have provided advantages such as lower processing temperatures, less stress, inexpensive materials, and amenability to rework (the replacement of defective components). Despite those advantages, serious problems have occurred in high-reliability devices. Their long-term solution requires understanding the chemical changes occurring on surfaces. Thus, we are collaborating with the Microelectronics and Satellite Reliability Groups to investigate the interaction of adhesives with other materials in the devices.

ANALYTICAL TECHNIQUES

Analytical techniques make use of a wide range of probes that interact with the surface to determine structure and composition. Electrons, ions, and photons have been used as excitation sources; each complements the others in revealing important features of the surface. The various sources and techniques used at APL for surface analysis are discussed below.

Electron Sources

The interaction of electrons with surfaces results in either elastic or inelastic processes. For elastic collisions, the backscattered electrons have the same energy as the incident (or primary) electrons. Elastically backscattered or diffracted electrons are frequently used to study surface structure. Under the appropriate experimental conditions, a low-energy (under 400 electronvolts) electron beam incident on a crystal surface is scattered by the surface atoms and produces a diffraction pattern on a fluorescent screen (Fig. 1), a method called low-energy electron diffraction. If the crystal surface is well ordered, the diffraction pattern consists of well-defined maxima that exhibit the symmetry of the surface layer. Detailed structural information about the surface can be obtained by correlating theoretical computations with the positions and intensities of the diffraction maxima.

Another low-energy electron diffraction technique, discovered at APL a few years ago,[1] involves the measurement of the total current absorbed by the sample as a function of incident azimuthal and polar angles of an electron beam (Fig. 2a). As the electron beam is rastered across the surface, images are obtained at constant beam energies and are displayed on a cathode ray tube. Diffraction patterns appear in these current images of the crystal surface (Fig. 2b) and the technique has been named current image diffraction. The process is discussed in greater detail in the section on Surface Structure Investigations Using Current Image Diffraction.

Inelastic collisions between the incident electron beam and the surface lead to several techniques that are used in surface analysis. As an example of inelastic scattering, a core electron, shown schematically in Fig. 3a, is ejected from an atom and is referred to as a secondary electron; the atom itself is left in an excited state. De-excitation can occur through two processes. In one, the excited atom can decay by emitting an X-ray photon, as shown in Fig. 3b, which is a one-electron decay process. In making the transition from the L level to the K level, an electron loses a precise amount of energy that appears as the X-ray photon. Alternatively, the atom can decay via a two-electron process in which an L-level electron makes a transition to the K level and a second atomic electron (say, one from the L level) is ejected with a specific amount of energy. The ejected electron is called an Auger electron; this de-excitation process is shown in Fig. 3c. Auger electron and X-ray photon emissions

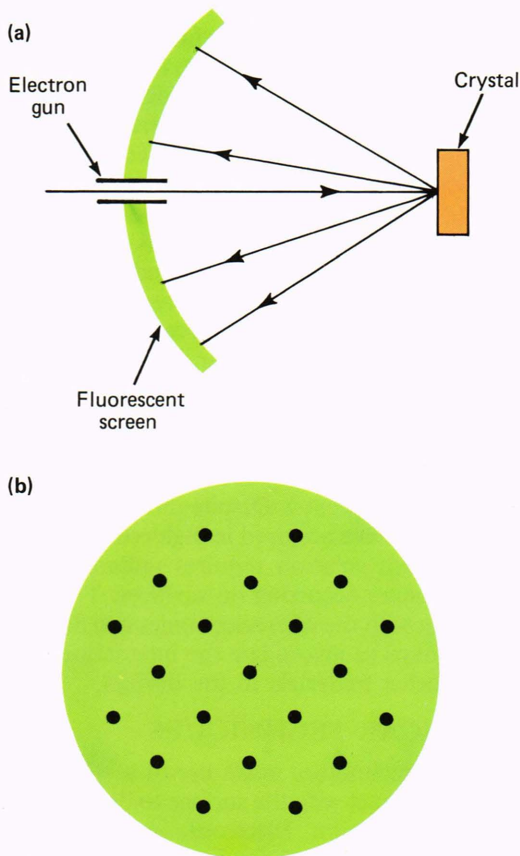

Figure 1—(a) Schematic diagram of a low-energy electron diffraction apparatus and (b) a low-energy electron diffraction pattern on a fluorescent screen.

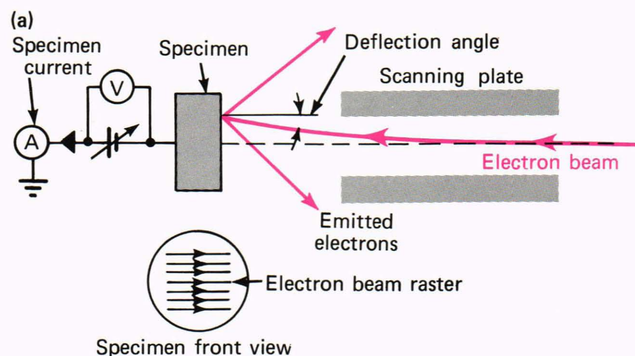

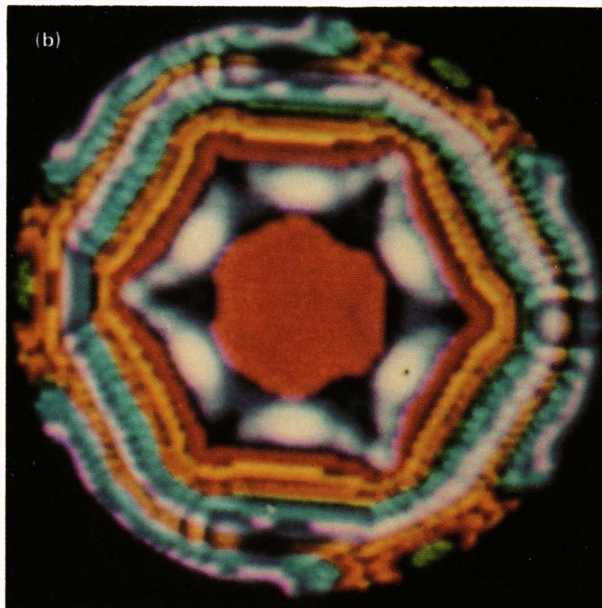

Figure 2—Schematic diagram of (a) the experimental apparatus for low-energy electron current image diffraction and (b) an idealized current image diffraction pattern of Al(111).

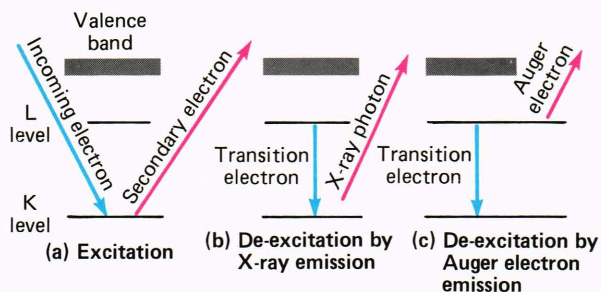

Figure 3—A schematic energy level diagram describing inelastic collisions of an electron with a surface atom. (a) Atomic excitation by an incoming electron, (b) de-excitation by X-ray emission, and (c) de-excitation by Auger electron emission. There are three resultant signals—a secondary electron, an X-ray photon, and an Auger electron—all of which are used prominently in surface analysis.

are competing processes, with the former favored by the lighter elements.

Scanning electron microscopy uses a highly focused electron beam at an energy from 2 to 30 kiloelectronvolts that is scanned over the sample surface. Secondary electrons emitted by the irradiated surface are especially useful for topographical imaging because they are relatively abundant and easy to collect. The technique is very sensitive to surface topography because the number of secondary electrons that are detected is strongly dependent on the incident illumination angle. Furthermore, because the yield of secondary electrons depends on material parameters such as work functions, images obtained by using secondary electrons also reveal contrast between different materials in the surface region.

X-ray photons that are emitted from a sample as shown in Fig. 3b are analyzed with a common accessory of a scanning electron microscope system, namely a solid-state detector/multichannel analyzer. Since the emitted X-ray photons have energies that are characteristic of the individual elements, the elemental composition of the near-surface region can be obtained by analyzing the energy spectrum of the X-ray photons. A common technique used for this purpose is called the energy-dispersive analysis of X rays, sometimes referred to as energy-dispersive spectroscopy. Energy-dispersive analysis of X rays is not strictly a surface analytical technique because the signals originate from the top 1 to 3 micrometers of the sample.

Auger electrons (Fig. 3c) escaping from an irradiated surface have proven to be extremely useful in surface analysis. A schematic diagram of an Auger electron spectrometer is shown in Fig. 4. The electron gun irradiates the sample with an electron beam having an energy from 1 to 5 kiloelectronvolts. The energy spectrum of the Auger electrons emitted from the sample is measured with a cylindrical mirror analyzer. After passing through the analyzer, the Auger electrons are detected with an electron multiplier. The detection of the weaker Auger electron signal in the presence of the strong secondary electron background is accomplished by differentiating the intensity versus energy curve for

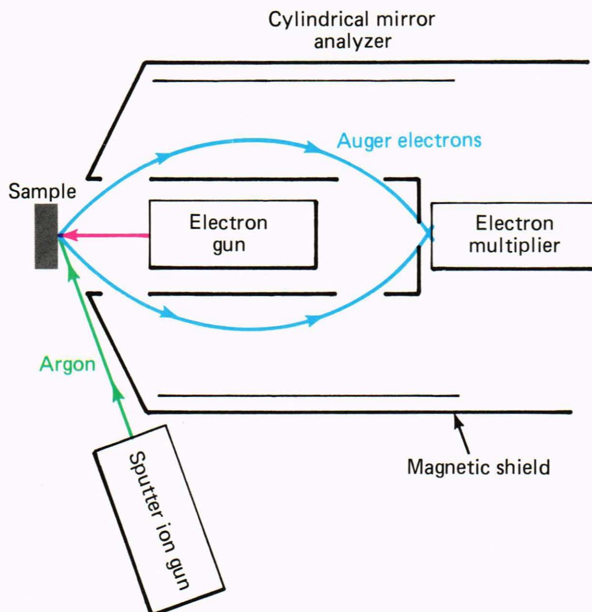

Figure 4—Schematic diagram of an Auger electron spectrometer. The energy spectrum of the Auger electrons emitted from the electron-irradiated sample is measured with a cylindrical mirror analyzer. The argon ion sputter gun is used to remove material from the sample surface to obtain elemental composition as a function of depth.

the emitted electrons, enabling the very sharp Auger peaks to be easily distinguished from the broad background.

The energy of the Auger electron is characteristic of the emitting atom and can therefore be used to determine elemental composition of the surface. With the exception of hydrogen and helium, all other elements can be detected by Auger electron spectroscopy with a typical sensitivity of about 1 percent of a monolayer and a spatial resolution of 3 micrometers for our instrument. The sampling depth is dependent on the energy of the emitted Auger electron which has a mean free path usually in the range of 4 to 20 angstroms. Thus, Auger electron spectroscopy is truly a surface-sensitive analytical technique. Elemental composition as a function of depth is obtained by sputtering (ion etching) the sample with argon ions. The sputtering process removes surface matter layer by layer, thereby continually providing a new surface for analysis.

Ion Sources

A technique that uses an incident beam of energetic ions (1 to 15 kiloelectronvolts) as the excitation source is secondary ion mass spectrometry. Elemental composition of a solid can be determined in both bulk and trace amounts for all elements down to the parts-per-billion range. Composition versus depth profiles are obtained as the sample is sputtered away during the analysis. APL's secondary ion mass spectrometer uses a duoplasmatron as the sputter-ion source; it is shown schematically in Fig. 5. A beam of primary ions (usually argon) strikes the sample with many ions penetrating

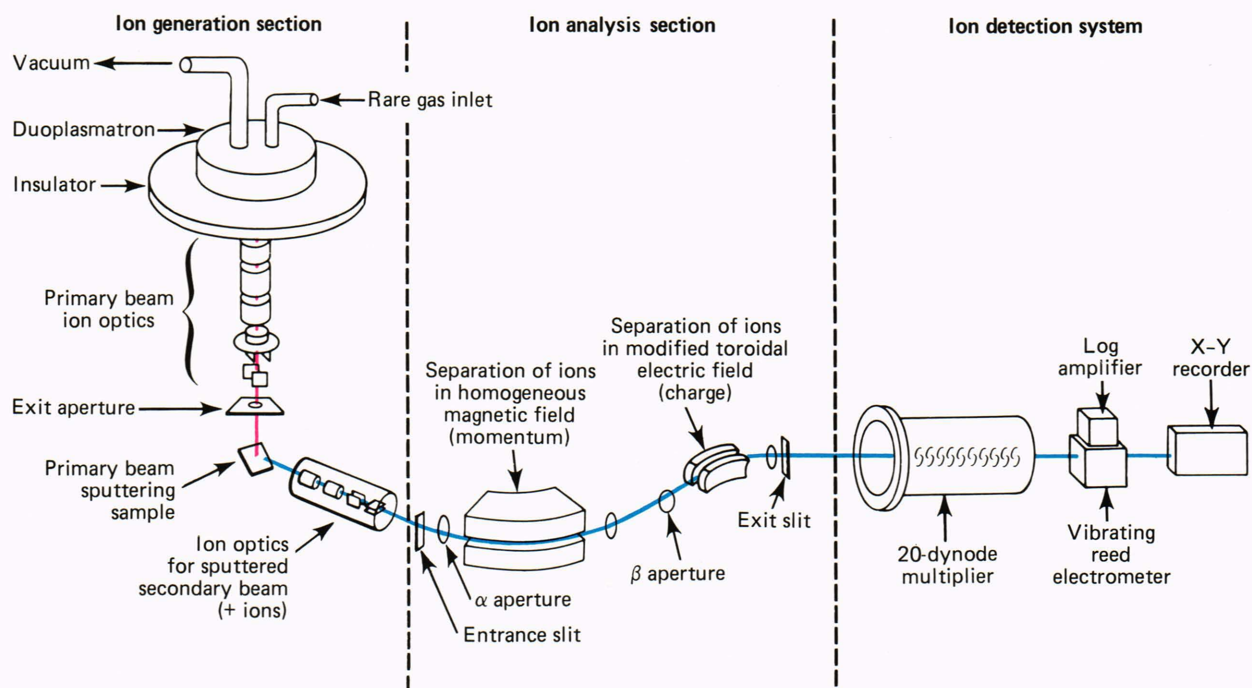

Figure 5—APL's sputter-ion source secondary ion mass spectrometer. The spectrometer is divided into three main sections: ion generation, ion analysis, and ion detection. A primary beam (red) from a duoplasmatron sputters a target, producing secondary ions (blue) that are extracted and focused onto the entrance slit of a double-focusing mass spectrometer (analyzer) and that exit onto the first dynode of a multiplier in the detection system.

the surface and exchanging momentum with the atoms of the sample. Chemical bonds in the path of entering ions are momentarily disrupted, resulting in the ejection of atoms, atom clusters, negative ions, and positive ions. The latter ions are formed into a secondary ion beam that is then analyzed in a mass spectrometer. In our instrument, the secondary ions are first separated by momentum in a magnetic field and then separated according to charge in an electric field, resulting in a spectrum of intensity versus mass-to-charge ratio of the ionic species.

The conversion of peak intensities to concentration can be a serious problem in secondary mass spectrometry because the ion yield of different species can range over several orders of magnitude. For example, oxides produce considerably higher ion yields than do metals, and sputtering with oxygen ions greatly enhances the ion yield.

Photon Sources

Techniques at APL that use photons as excitation sources are infrared and Raman spectroscopy. In infrared spectroscopy, photons transmitted or reflected by the sample are measured as the wavelength is scanned from 2.5 to 30 micrometers, a spectral region that corresponds to the interatomic vibrational energies of molecules and molecular materials. Because most materials have a unique set of vibrational energies, the corresponding infrared absorption spectrum can be used to determine the molecular composition of the sample. Raman spectroscopy is also sensitive to the vibrational modes of the sample, but it is a true scattering process. Because their physical mechanisms differ, infrared and Raman spectroscopy provide complementary information about materials.

The most common light-scattering processes involving molecules are illustrated in Fig. 6. Incident photons at frequency ω_0 interact with molecules and are scattered over 4π steradians with elastic and inelastic components. The elastic scattering, referred to in the past as Rayleigh scattering, is the phenomenon that results in the blue appearance of the sky and the red sun at sunrise and sunset (because the shorter wavelength blue light is scattered more strongly than red). Because the process is elastic, the scattered light is of the same frequency as the incident light; it is not specific to the molecule causing the scattering.

The inelastic scattering of light by molecules is known as spontaneous Raman scattering and is termed rotational, vibrational, or electronic, depending on the nature of the energy change that occurs in the molecule. Because only one photon in 10^6 to 10^8 is inelastically scattered, the Raman bands are many orders of magnitude weaker than the elastically scattered light. As illustrated in Fig. 6, Raman scattering consists of weak components at fixed frequency separations on both sides of ω_0. The frequency separations are related to the characteristic frequencies of the molecule, as, for example, the vibrational frequency, ω_v, in Fig. 6. The Raman component that is displaced toward a longer wavelength is known as the Stokes band (ω_s) and that toward a shorter wavelength as the anti-Stokes band

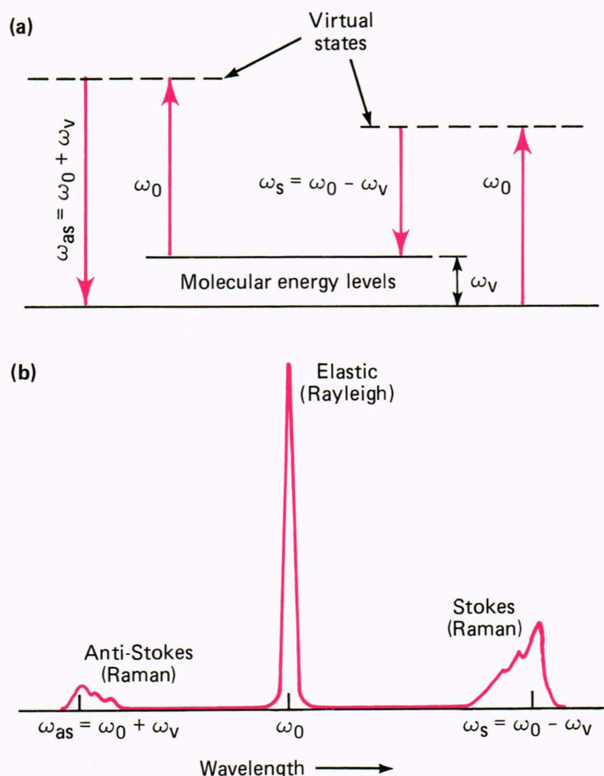

Figure 6—Spontaneous Raman scattering. (a) Energy level diagram and (b) spectrum. The intensities are not to scale; the Raman bands are actually much weaker.

(ω_{as}). The Stokes band arises from molecules in the ground vibrational state, whereas the anti-Stokes band arises from molecules in higher vibrational levels. Because most molecules at room temperature are initially in the ground vibrational state, the Stokes band is much stronger than the anti-Stokes band. Thus, in practice, only the Stokes side of the spectrum is scanned in spontaneous Raman scattering.

The Raman bands are the result of a true scattering process; i.e., the incident photons are not absorbed and re-emitted as in fluorescence. Hence, any incident wavelength can be used as long as $\omega_0 > \omega_v$, although visible radiation is preferred because of the high sensitivity of detectors in the visible region and the fact that the intensity of the Raman scattering scales as ω_0^4. In vibrational Raman scattering, the interaction between the radiation and the sample depends on the vibrational modes of the molecule and is, therefore, species specific. In addition to the ω_0^4 dependence, the Raman scattering intensity is linearly proportional to the species number density and the intensity of the incident light. Because of the latter, it was not until the advent of high-power lasers that Raman scattering became a practical method.

SURFACE STRUCTURE INVESTIGATIONS USING CURRENT IMAGE DIFFRACTION

As mentioned previously, in our surface structure investigations of several metal and semiconductor surfaces, we have used the current image diffraction method (Fig. 2). An electron beam is rastered across the surface of a crystal sample, and images are obtained from the leakage current absorbed in the sample from the beam. The surface is imaged by a scanning electron beam that strikes the sample at constantly varying azimuthal and polar angles. The sample current is measured at every position where the beam strikes the surface and is displayed synchronously on a cathode ray tube. In these current images of the crystal surface, diffraction patterns appear as changes in contrast caused by variations of the total reflectivity of the crystal surface with the incident angle of the electron beam.

Single crystals can be cut along various crystallographic directions to form surfaces consisting of planes of atoms that exhibit symmetries characteristic of the particular planes. Planes of atoms of various orientations and directions in single crystals are indexed by a set of three integers called Miller indices, designated (h, k, l).

Surface information that can be derived from current image diffraction measurements includes crystal orientation and symmetry, interplanar spacings, the inner potential (potential felt by the electron upon entering the crystal field), and adsorbed layer structure. An example of adsorbed layers affecting the current image diffraction patterns is shown in Fig. 7 for oxygen adsorption on the Al(111) surface.[2] The pattern for the "clean" surface (no oxygen adsorbed) had a hexagonal set of dark spots centered at an angle of incidence of 4.5 degrees, a trigonal set of dark spots at 9 degrees, and additional structure at larger angles. Dark spots in the figure correspond to regions of smaller adsorbed current through the sample. As a function of oxygen exposure, the set of hexagonal spots faded and were nearly gone by 140 langmuirs, leaving only the trigonal spots (1 langmuir is the exposure of a surface to a gas at a pressure of 10^{-6} torr for 1 second). Since the effect of oxygen adsorption was to alter only the relative intensities of backscattered electrons and not to affect the spot geometry, this suggested that oxygen was being adsorbed as an ordered overlayer, which is in agreement with other studies. In contrast to this, current image diffraction patterns for the surface parallel to the (100) plane, Al(100), uniformly degraded with oxygen coverage indicating a non-ordered adsorption process.[1] Thus, from these measurements, it is possible to obtain structural information about the oxygen adsorbed layer.

Other features observed in the current image diffraction patterns have been attributed to electron channeling[3] and to electrons being scattered alternately by the outermost plane of atoms and the surface potential barrier.[4] Electron channeling is the elastic scattering of electrons from planes of atoms near the surface. An example is shown in Fig. 8a for current image diffraction of the Ti(001) surface. Channeling effects are manifested as line features in current image diffraction patterns. These features have been identified as Bragg or Laue scattering from specific atomic planes.[3,5] The channeling pattern, calculated with Bragg theory for

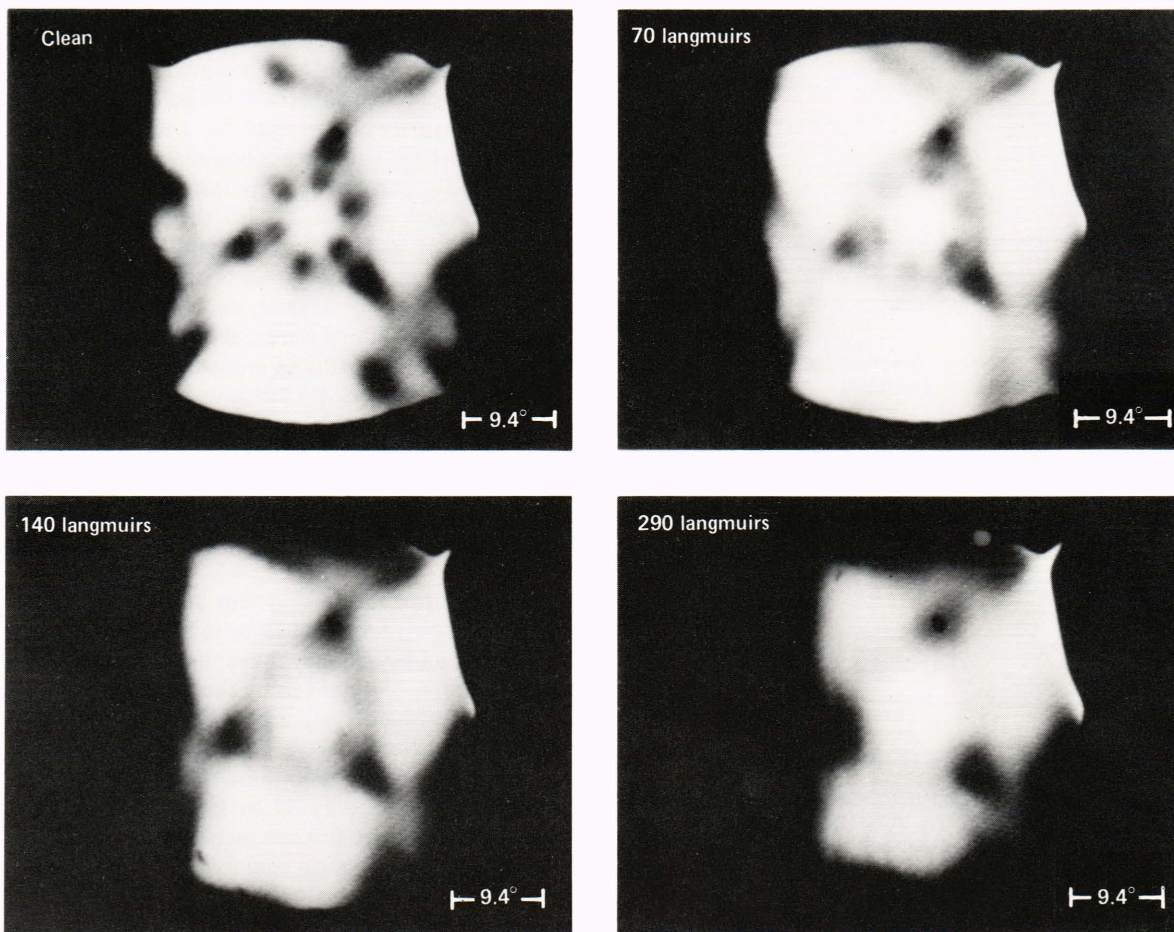

Figure 7—Current image defraction patterns of the Al(111) surface as a function of oxygen exposure for a beam energy of 20.8 electronvolts relative to the vacuum. The exposures, as indicated on each photograph, were clean, 70, 140, and 290 langmuirs. Angles are measured from the center of the pattern.

Figure 8—(a) Experimental pole-crossing of the lines due to Bragg scattering from the {114} planes of the Ti(001) surface at a primary beam energy of 61 electronvolts relative to the vacuum. (b) Calculated pattern of the same lines assuming the bulk lattice constants and an inner potential of 12 electronvolts.

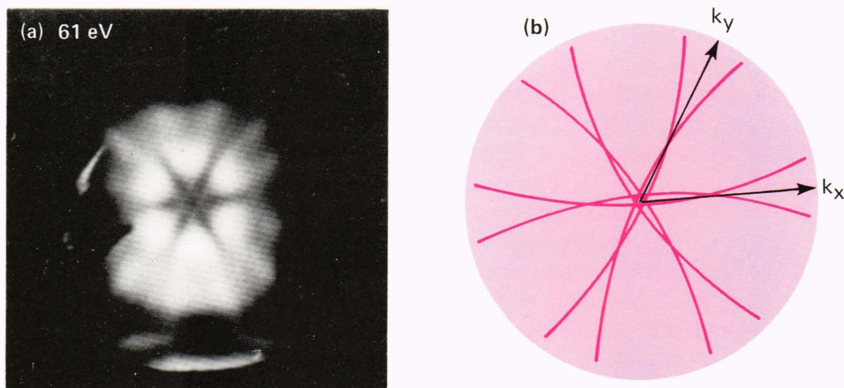

scattering from the {114} set of equivalent planes, is shown in Fig. 8b for a primary beam energy of 73 electronvolts relative to the zero of the inner potential. The agreement between the predicted line positions and the experimental image at a beam energy of 61 electronvolts with respect to the vacuum is quite good and corresponds to an inner potential of 12 electronvolts, a reasonable value for this quantity. The spot patterns in Fig. 8a can be reproduced by a computation of the total reflectivity using a dynamical theory. If the inner potential is known, the channeling patterns can be used to determine the planar spacing near the surface with little computational effort, which is in marked contrast to low-energy electron diffraction experiments. In the latter method, the distances between planes of atoms near the surface are determined by comparing spot intensities of several low-energy electron diffraction beams with a complex theoretical analysis that depends

on a number of adjustable parameters, some of which are structural parameters and some are not. On the other hand, the theoretical analysis required to interpret the current image diffraction patterns is much simpler and more straightforward because it involves only computations of line positions and not intensity. Furthermore, there are only two adjustable parameters, the planar separation and the inner potential. This is a major advantage of the current image diffraction method, and it is being exploited in measuring structural parameters of selected crystals.

Another feature that has been observed in the current image diffraction patterns has been interpreted as a result of evanescent diffracted electron beams, which are beams of electrons that are diffracted into the crystal and attenuated due to inelastic scattering. At a constant primary electron beam energy and direction, only a few diffracted beams can leave the crystal. As the primary beam energy increases, the number of electron beams diffracted out of the crystal increases. Also, as the angle of incidence of the primary beam varies, the number of diffracted beams out of the crystal can change. The primary beam energy and the incident angle at which a new beam emerges from the crystal are termed the onset of evanescence. At a primary beam energy and incident angle just below the onset of evanescence, the pre-emergent evanescent diffracted electron beam is traveling almost parallel to the crystal surface. This pre-emergent beam interferes with the primary electron beam, resulting in very sharp lines or features in the current image diffraction patterns.

Displayed in Fig. 9 is a series of four images obtained from the (100) face of aluminum that has fourfold symmetry as is clearly seen in the diffraction patterns. At 13 electronvolts, the evanescent curves are seen as double lines of dark contrast approaching the image center from the four ⟨1,0⟩ directions ([1,0], [$\bar{1}$,0], [0,1], and [0,$\bar{1}$]). At 15.5 electronvolts, the first set of dark curves is crossing the center, and, at 18.0 electronvolts, the second set is crossing. At 17.0 electronvolts, the white line between the sets of dark curves is crossing. This phenomenon can be better observed in the individual current profiles in the [0,1] direction, as shown in Fig. 10. In the current traces, maxima cor-

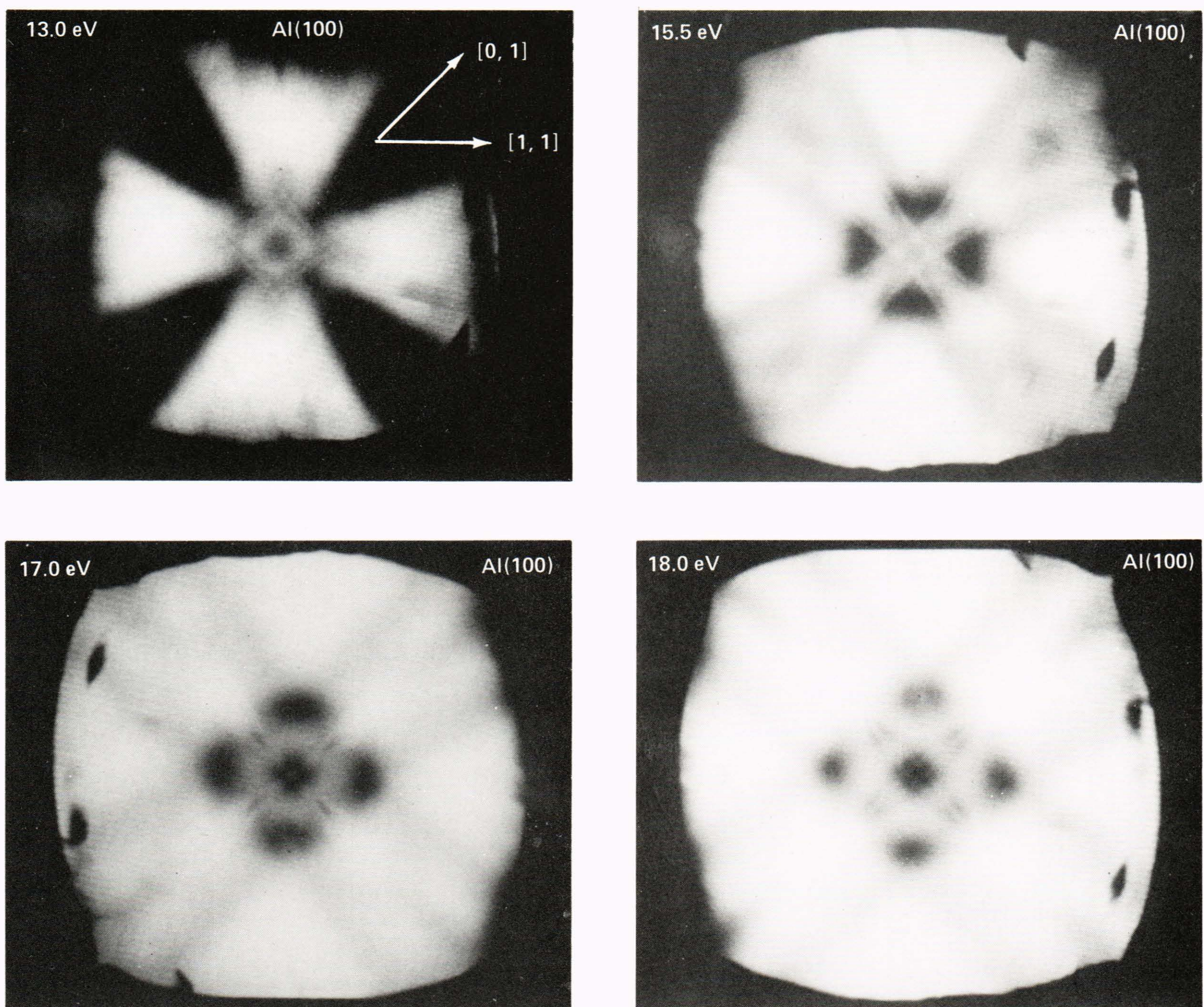

Figure 9—Four low-energy diffraction patterns showing lines due to beam evanescence approaching and crossing the center of the image.

respond to areas of light contrast in full images whereas minima are regions of dark contrast. Evanescent profiles such as those observed in Figs. 9 and 10 can be distinguished from other line features by their spatial narrowness and energy dependence. Three-dimensional channeling lines shown in Fig. 8 are much broader. Lines resulting from diffraction beam evanescence have also been identified on the (110) and (111) surfaces of aluminum.

We are continuing to make progress in understanding the features observed in the current image diffraction patterns, which should lead to quantitative information about surface structure. For example, the technique should be useful in studying surface relaxation, which is the phenomenon that the interplanar spacings near the surface are different from the bulk values because the surface atoms are in a different environment; i.e., they are exposed to different electrostatic potentials.

SURFACE/MATERIALS INVESTIGATIONS IN MICROELECTRONICS

The performance and reliability of electronic devices are very dependent on surface phenomena and the properties of materials. In this area, our emphasis has been on investigations of the properties of organic adhesives that are used for die (chip) and substrate attachment in microelectronic devices. Especially when high reliability is required, serious problems can occur when using organic adhesives,[6-9] including: mechanical problems such as the loss of adhesion and thermal mismatch; electrical problems such as open circuits or, when conductive adhesives are used, the resistance variation with time or temperature; short circuits that result from the electromigration of metal, especially silver, from conductive adhesives; and finally, chemical problems because of the interaction of the adhesive with other materials in the device. Chemical species, both volatile and nonvolatile, evolve from the adhesive during and after cure. Metals may be corroded, wire bonds may be weakened, or the adhesive may be degraded by cleaning or thermal procedures. Furthermore, moisture adsorbed by the adhesive may lead to eventual failure. Very little is known about the complex chemical species that evolve from adhesives, their adsorption, or their interaction with other materials.

Failure Modes in Hybrid Microcircuits

Current examples of the useful application of surface analytical techniques include failure studies in hybrid microcircuit devices for cruise missiles. (This is a collaborative effort with the Microelectronics and the Satellite Reliability Groups and the Fleet Systems Department.) The failure mechanisms need to be understood so that fabrication procedures can be modified to improve the reliability of the devices. The failures were caused by electrical current leakage that falsely turned on relay drivers. Failures occurred at both hot

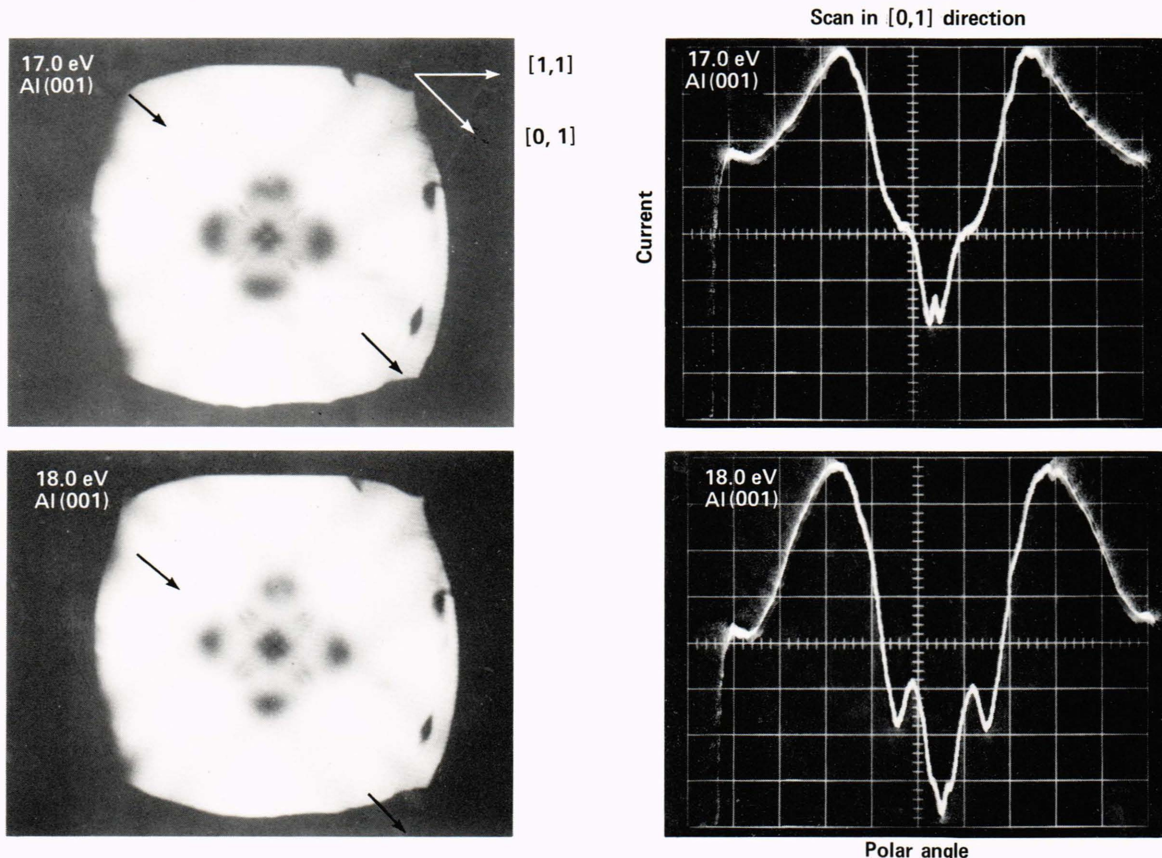

Figure 10—Diffraction images and corresponding current profiles in the [0,1] direction at low beam energies. Maxima in the current profiles correspond to areas of light contrast in the patterns. Minima are dark regions.

and cold test temperatures and were not always repeatable, which probably indicated that there were multiple failure mechanisms. The cold-temperature failures were correlated with excessive amounts of ammonia in the package. Presumably when the dew point of ammonia was reached, ionic contaminants were dissolved in the liquid ammonia, thereby providing a conductive medium. It was suspected that the high-temperature failures may have been caused by high levels of hydrocarbons, ammonia, and moisture in the package that adsorbed on the surface and increased the conductivity between regions that should have been electrically isolated.

Shown in Fig. 11 are maps of the carbon and oxygen distributions on the surface of a transistor in a hybrid that failed during the temperature cycle testing due to an electrical short between the emitter and the collector. The elemental maps were obtained with the Auger electron spectrometer by setting the analyzer for the Auger electron energy of the desired element and scanning the electron beam across the surface. High levels of surface concentration correspond to light areas in the photographs. Figures 11b and 11c show that a continuous track of a contaminant containing carbon and oxygen was present between the emitter and the collector, which may have been responsible for the short. The contaminant may have been an outgassing product from the epoxy used for the substrate attachment. Fabrication procedures could also have contributed to the contamination. Use of a newer, higher purity, lower outgassing epoxy to attach the substrate to the package has resulted in a much lower failure rate.

A longer term failure mode was found to involve the electromigration of silver away from the conductive epoxy used to attach the transistors and diodes to the substrate. Migration of silver was observed by scanning electron microscopy on the insulating ceramic substrate between conductor tracks (Fig. 12) and up the sides and across the top surface of the transistors (Figs. 13 and 14). From previous electromigration studies of conductive epoxies, it is known that the presence of an electrolytic medium (usually water) greatly increases the rate of electromigration. The excessive levels of ammonia in these hybrids might have provided the conductive medium. Additional research using controlled experiments is needed to establish the specific conditions that lead to electromigration.

Elemental Composition of Adhesives

It is clear from the above discussion that experiments are needed to determine the composition of cured adhesives and to identify the volatile and adsorbed species that are evolved and that may be potential sources of contamination. We have used secondary ion mass spectrometry to determine the elemental composition of several adhesives that are widely used for die attachment. During the analysis, sputtering was continued until successive spectra were essentially the same, which indicated bulk composition. A typical spectrum of a conductive adhesive is shown in Fig. 15. Of particular importance are the levels of Na, K, and Cl, which, if

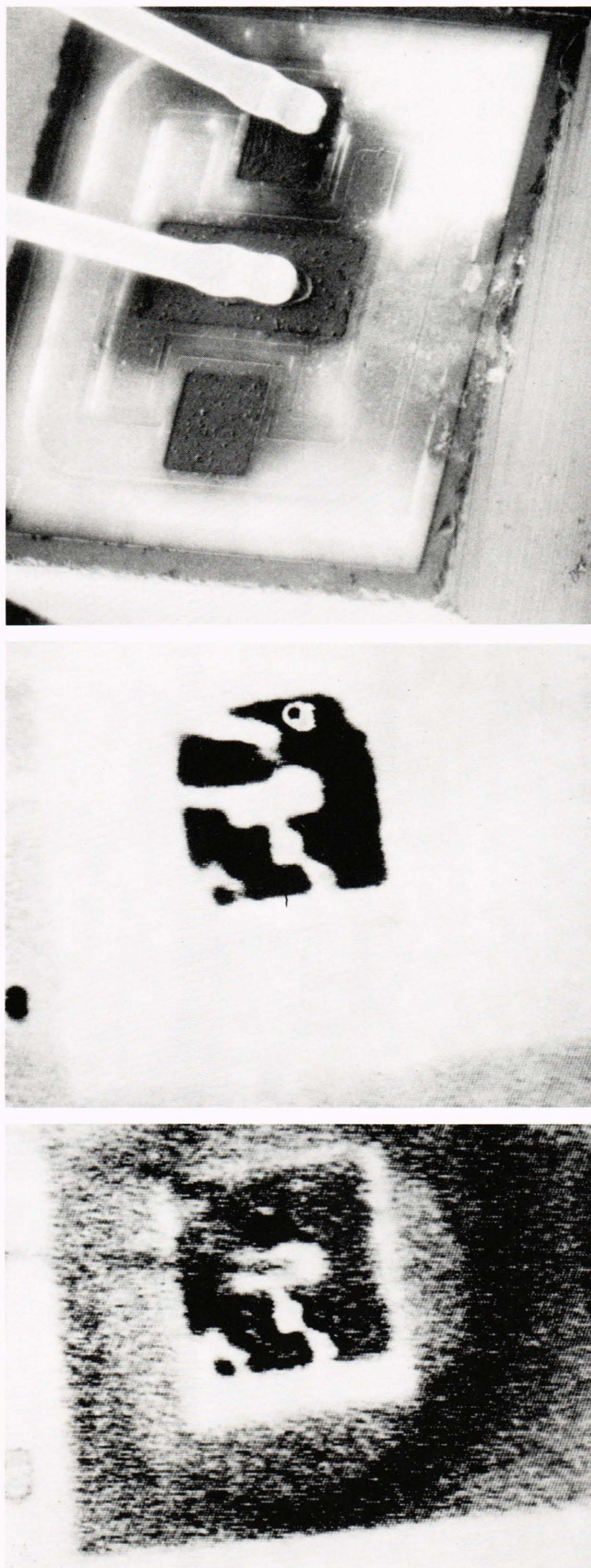

Figure 11—2N2222A transistor in failed hybrid. Top: Secondary electron image; middle: Auger carbon map; and bottom: Auger oxygen map.

mobile and at sufficiently high concentrations, can lead to device failures. Because of this potential problem,

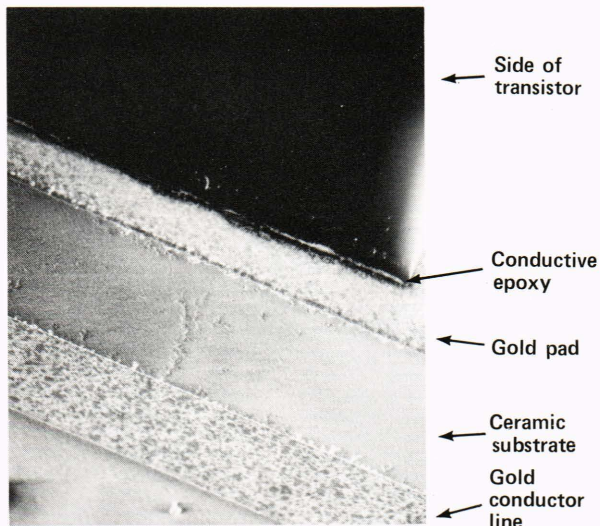

Figure 12—Scanning electron microscope photograph of failed hybrid, showing silver electromigration across the gold transistor pad and ceramic insulator gap to the gold conductor line; 28 volts were applied across the 127-micrometer insulating region.

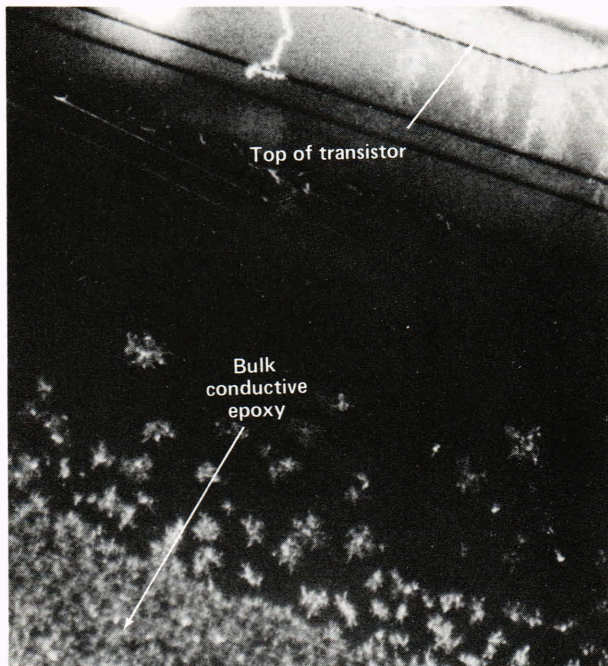

Figure 13—Scanning electron microscope photograph of failed hybrid, showing silver electromigration up the sides and across the top of a 2N2222A transistor.

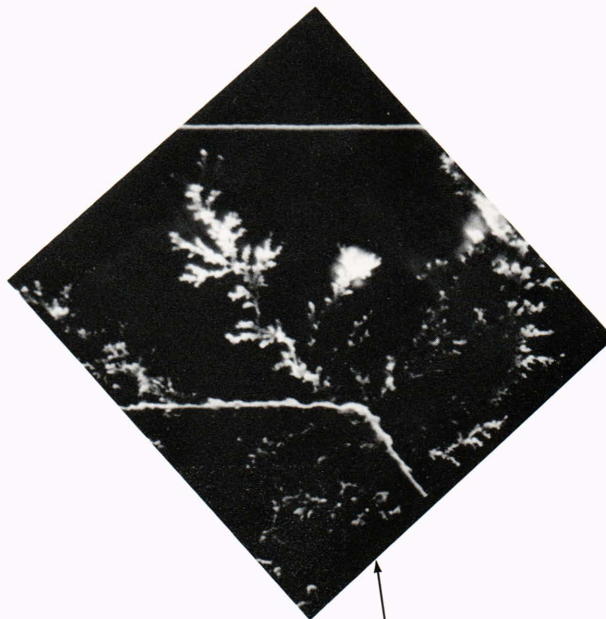

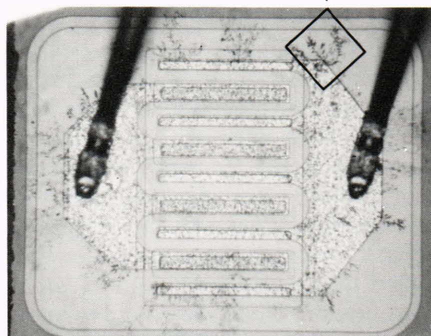

Figure 14—Top of the 2N2222A transistor in a failed hybrid. Note the dendritic growth of the silver, which is light in the scanning electron microscope photograph (top) and dark in the optical photograph (bottom).

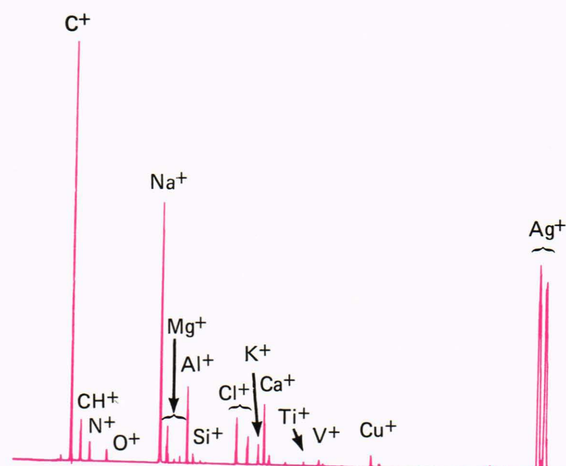

Figure 15—Secondary ion mass spectrum of Ablebond 36-2 epoxy adhesive.

the new military specification for adhesives requires that extractable ion levels be below certain limits as measured by ion chromatography.

Adsorbed Species from Adhesives

During the fabrication of hybrids for the Galileo spacecraft, wire bond problems were encountered that involved low-temperature, impurity-driven intermetallic growth when two different epoxies (Ablefilms 517 and 550) were cured simultaneously in the same package.[10] The wire bond problems occurred only after burn-in (the device heated for 240 hours at 125°C).

When either epoxy was used individually, no problems were encountered. This suggested that chemical species from both epoxies might have a synergistic effect. The wire bond problems were thought to be due to the adsorption of these chemical species on the aluminum bonding pads. In the earlier work,[10,11] no definitive results were obtained regarding adsorbed species originating from the epoxies. The issue has been reexamined with improved sensitivity.[12] Thin-film aluminum-on-silicon substrates, exposed to the epoxies during cure, were analyzed using Auger electron spectroscopy and secondary ion mass spectrometry. The Auger spectra of the substrates exposed to the cure of the epoxies are shown in Fig. 16. Essentially no adsorbed species were detected (the carbon signal was barely above the noise level) during the cure of Ablefilm 517 (Fig. 16a), while a rather large carbon signal and possibly a trace of nitrogen were detected on the substrate that was exposed during the cure of Ablefilm 550 (Fig. 16b). It is known[11,13] that Ablefilm 550 outgasses more organic species than Ablefilm 517. The nitrogen species may have been from the amine curing agent. No additional elements nor increases in the carbon and nitrogen signals were observed when Ablefilms 517 and 550 were cured simultaneously. Hence, no synergistic effects were observed. Experiments with a covered epoxy layer at one end of the metallized substrate suggested that surface diffusion was a significant factor in the transport of species originating from the epoxy. Secondary ion mass spectrometry measurements were in general agreement with the Auger results. Because of the much higher sensitivity of the secondary ion mass spectrometry technique, additional contaminants were detected in the aluminum oxide layer of both the control and the test substrates. Thus, these species were associated with the metallization, not the epoxy adhesives.

It should be noted that a limitation of both the Auger method and secondary ion mass spectrometry is that the information obtained is primarily elemental as opposed to molecular. In the future, we plan to conduct multichannel Raman and X-ray photoelectron spectroscopic experiments to determine the molecular identity of adsorbates. This is essential in determining the source of a contaminant and in understanding how adsorbed species interact with surfaces.

Volatile Species from Adhesives

Volatile species that evolve from adhesives during and after cure are measured mass spectrometrically. The mass spectrum of the outgassing products during the cure of an epoxy adhesive is shown in Fig. 17. The main constituents (Fig. 17a) appeared to be parent and fragment ions of methyl alcohol, nitrogen, carbon dioxide, ammonia, water, and possibly acetone. Higher mass species that appear at low concentrations (Fig. 17b) were probably associated with the modified epoxy resin.

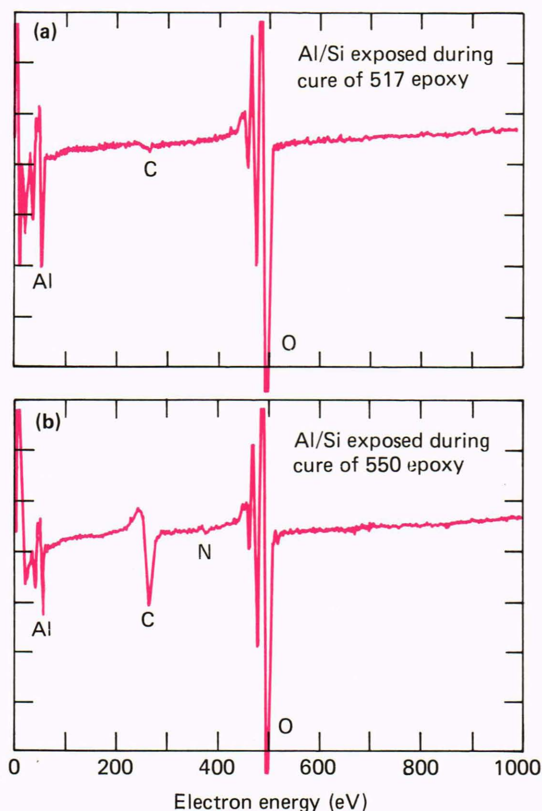

Figure 16—Auger spectra of aluminum-on-silicon substrates placed near epoxy samples during cure at 150°C for 2 hours. The substrates were cleaned with ultraviolet/ozone prior to the experiment.

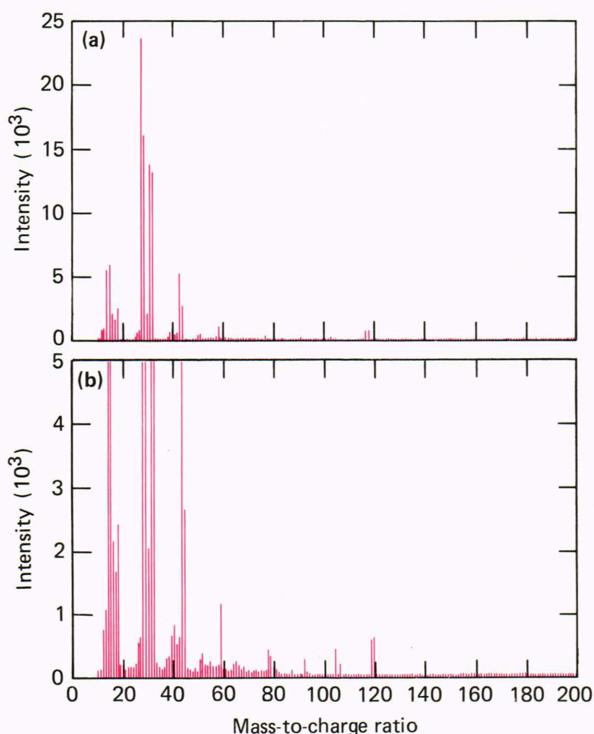

Figure 17—(a) Mass spectrum of volatile species produced during the cure of Ablefilm 550 epoxy at 150°C in helium. The pressure in the mass spectrometer was 1.1×10^{-5} torr. The intensity scale has been expanded in (b) to show the smaller peaks.

After a 24-hour vacuum bakeout at 125°C, the epoxy samples were heated in vacuum at 125°C for extended periods. The same principal outgassing products were observed as above, with carbon dioxide becoming the dominant species at later times. Higher mass species were evolved throughout the heating period, although the relative composition changed with the heating time. Due to the complexity of the mass spectrum, the higher mass species could not be identified. In the future, we will use a gas chromatograph to separate the chemical species before they enter the mass spectrometer, thereby simplifying the mass spectrum and making it easier to identify the species.

ANALYSIS OF CONTAMINANTS

As in the hybrid microelectronics work discussed above, contamination can be a severe problem in other areas, particularly in spacecraft where high reliability is essential. Recent examples of problems on which we have collaborated with the Space Department include contamination of integrated circuit packages, space simulation chambers, and sensitive satellite sensors.

Integrated Circuit Packages

In addition to internal contamination, contamination on the outside of microelectronic packages and on circuit boards can be a source of difficulty. Raman spectroscopy was used to identify contaminants present on an integrated circuit that developed an electrical short between adjacent leads after hot/cold testing. Initial optical and scanning electron microscopic investigations showed a residue between two of the integrated circuit leads, and X-ray analysis showed an excessive concentration of sodium in the suspect area. From these results, it was hypothesized that the contaminant might be a residue of the acoustic couplant used in the particle impact noise detection test. The specific couplant, Sperry type 50A408, was known to contain glycerol and sodium tetraborate.

A Raman spectrum (Fig. 18a) using the 488-nanometer line of an argon ion laser was obtained of the contaminant between the integrated circuit leads and compared with the spectrum (Fig. 18b) taken on an uncontaminated portion of the same integrated circuit. The Raman spectrum of the Sperry couplant (Fig. 18c) was very similar to that of the contaminant, and it was concluded that the contaminant was indeed from the test couplant. Finally, it was shown that the Raman bands of the contaminant were largely due to glycerol (Fig. 18d).

It was conjectured that, following the test, the integrated circuit was incompletely rinsed with water and not all of the ultrasonic couplant was removed; when the excess water evaporated, a conductive residue remained. The degree of conductivity was determined by the amount of water bound to the hygroscopic residue.

Space Simulation Chambers

It is essential that space systems not be contaminated during the extensive testing that is required to qualify the systems for launch. This is particularly important with optical components or sensitive detectors because their performance could be severely degraded from the original design goals. Infrared spectroscopy was used to identify contaminants in the Space Simulation Laboratory at APL. Three samples of unknown composition were analyzed.

Sample No.1 was a greasy deposit around the ports of the chamber. Sample No. 2 was an oily residue at

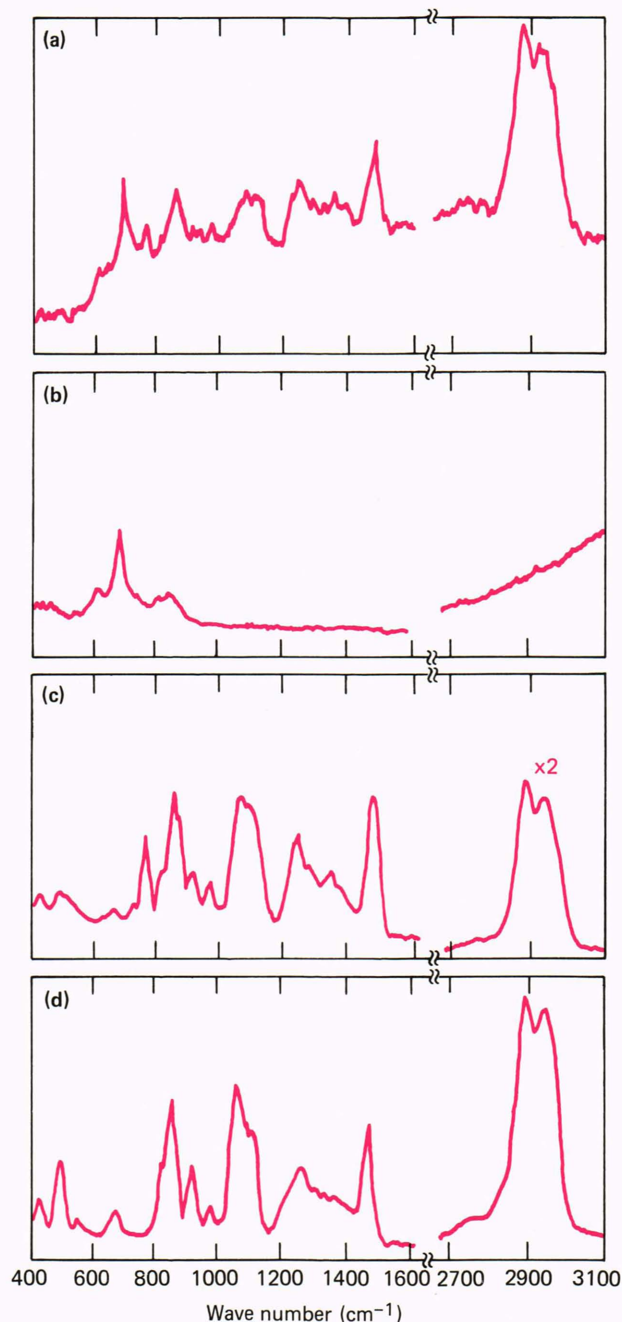

Figure 18—Raman spectra obtained with an argon laser at 488 nanometers, 100 milliwatts: (a) contaminated region on integrated circuit package; (b) uncontaminated region on same package; (c) Sperry 50A408 ultrasonic coupling gel; and (d) glycerol.

the bottom of the chamber. Sample No. 3 was material that condensed on an iridium witness plate during a cooling test (a sample that is analyzed before and after a test to determine if the test affected it).

The infrared spectrum of sample No. 1 is shown in Fig. 19a. Comparison with infrared spectra of suspected materials that may have been the source of the contamination indicated that the greasy deposit was a mixture of bis(2-ethylhexyl)phthalate (used in some types of diffusion pump oils) and Dow Corning high-vacuum grease or Dow Corning 4 compound. The spectra of these known materials are shown in Figs. 19b, 19c, and 19d. It was similarly shown that sample No. 2 was mainly bis(2-ethylhexyl)phthalate, and the infrared spectrum of sample No. 3 was consistent with the spectrum of a saturated linear hydrocarbon.

It was concluded that the chamber had been contaminated with Octoil diffusion pump oil, mechanical pump oil, and Dow Corning high-vacuum grease or 4 compound. Discussions with Space Simulation Laboratory personnel revealed the probable sources of these contaminants. These investigations point out the need for periodic analysis of witness plates for an accurate evaluation of the cleanliness of test chambers.

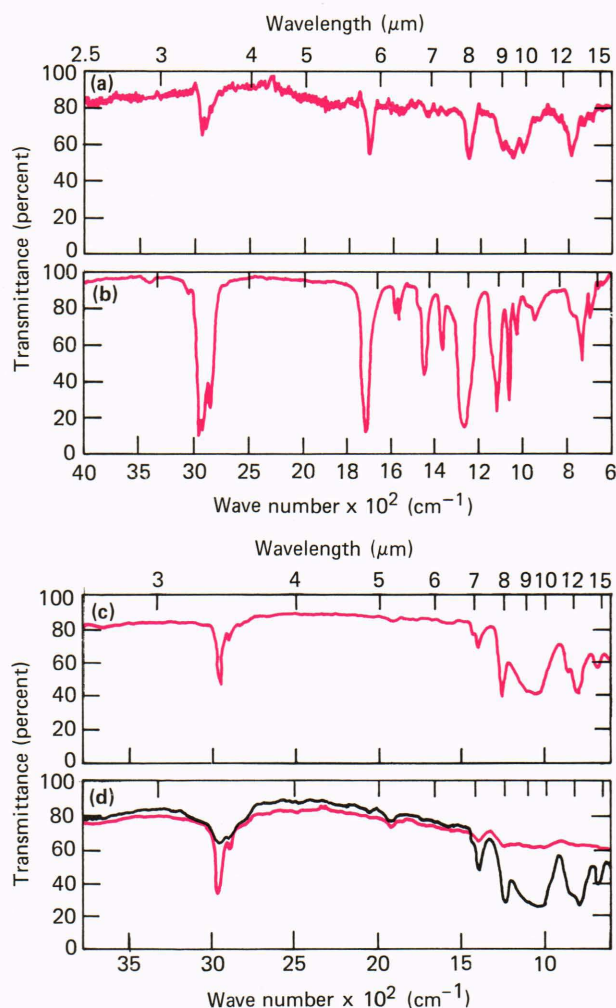

Figure 19—Infrared spectra. (a) Sample No. 1, greasy deposit around ports in Space Simulation Laboratory, (b) bis(2-ethylhexyl)phthalate (Octoil diffusion pump oil), (c) Dow Corning high-vacuum grease, and (d) Dow Corning 4 compound. Note that the wavelength scale of (a) and (b) is different from that of (c) and (d).

The Disturbance Compensation System

The third example of the analysis of contaminants involves the Disturbance Compensation System (DISCOS). After launch of the NOVA satellites, it was observed that the proof mass in DISCOS was subjected to anomalous forces. These forces gradually decreased over a several month period, but, because the forces changed with time, sometimes unpredictably, they prevented the accurate and reliable prediction of satellite position for the desired eight-day interval. Hence, the satellites were unable to achieve their full operational capability until the anomalous forces decreased significantly. It was postulated that outgassing within the DISCOS cavity may have been responsible for these forces. In particular, the Lexan end-caps were believed to be the primary outgassing source because of previous measurements on the outgassing of water from Lexan.

The composition of the DISCOS outgassing material was measured mass spectrometrically using a previously baked-out stainless steel chamber. The major species evolved at 25 and 60°C were nitrogen, oxygen, water, carbon dioxide, and argon; the latter came from the test chamber, which was purged with argon during the loading of DISCOS. Several organic compounds and Freon 113, which was used to clean some of the components prior to assembly, were detected at low concentrations.

Several of the materials used in the fabrication of DISCOS were individually studied to determine their particular outgassing characteristics and to compare with the outgassing of the assembled unit. The major sources of water in DISCOS were found to be outgassing of Lexan and G-10 Epoglass. The main source of carbon dioxide was the Eccofoam, which has the gas trapped in the cellular structure of the foam. The nitrogen may have been a result of prior storage of the sensor in nitrogen since none of the materials that were studied outgassed significant quantities of nitrogen.

MISSILE APPLICATIONS

Because the materials in missiles are subjected to very high temperatures and oxidizing environments, there is a continuing effort to develop new materials that will survive under unusually severe conditions. We have been collaborating with the Aeronautics Department on the evaluation of such materials. An example concerns the analysis of thoriated tungsten nozzle inserts that developed cracks during test firings.

Scanning electron microscopy and Auger electron spectroscopy were used to help determine the cause of large cracks that developed in 2 percent thoriated tungsten exit cone and throat inserts in nozzles that were exposed to very-high-temperature flowing gases during tests. The investigation revealed cavities and areas in

which thorium was concentrated in the vicinity of the crack tips as shown in Fig. 20. A possible explanation was the formation of tungsten carbide. The melting point of 2 percent thoriated tungsten is approximately 6100°F, whereas the eutectic melting point of tungsten carbide is only 4487°F. Thus, the carbide phase could have been liquid with gas bubbles in it while the surrounding material was still solid. This would explain the presence of the cavities. The source of the bubbles could have been the combustion gases or the hydrogen released when the hydrocarbon gases from the charring phenolic combined with the tungsten to form tungsten carbide. The formation of liquid tungsten carbide might also explain the separated thorium because the dispersed thorium could have separated out and become concentrated when the carbide was formed.

CONCLUDING REMARKS

In this article, surface analytical techniques were reviewed together with examples of their applications to several areas of interest at APL. The current image diffraction method developed at APL provides a new approach in determining surface structure and offers a major advantage in that the theoretical interpretation of the data is simpler and more straightforward than in low-energy electron diffraction experiments. The microelectronics applications demonstrate the utility of advanced analytical techniques in determining the causes of failures in devices and in providing information about the physical and chemical properties of materials that are used in microelectronics. From this knowledge, higher production yields of devices are attainable and performance and reliability are improved. In spacecraft applications, advanced analytical techniques enable low-level contaminants to be analyzed and their sources determined, which then allows corrective action to be taken. Surface techniques were also shown to be very useful in evaluating materials that are being developed for missile applications.

Improvement in surface science facilities continues to open up new areas of investigation. A sample introduction system and preparation chamber is being added to the Auger electron spectrometer that will enable samples to be loaded without disturbing the ultra high vacuum in the main chamber. In the new chamber, samples can be cleaned, heated, analyzed, and subjected to gases under controlled conditions so that adsorption, desorption, and surface chemical reactions can be investigated. A multichannel Raman spectrometer will be able to probe adsorbates on a molecular level to determine their identity and their interaction with surfaces. Molecular information will complement the elemental information obtained from Auger analysis and secondary ion mass spectrometry. Finally, the addition of a gas chromatograph to the mass spectrometer system for analyzing volatile outgassing products from materials will enable species to be separated before they enter the mass spectrometer, thereby simplifying the analysis of complex mixtures.

REFERENCES

[1] B. H. Nall, A. N. Jette, and C. B. Bargeron, "Diffraction Patterns in the

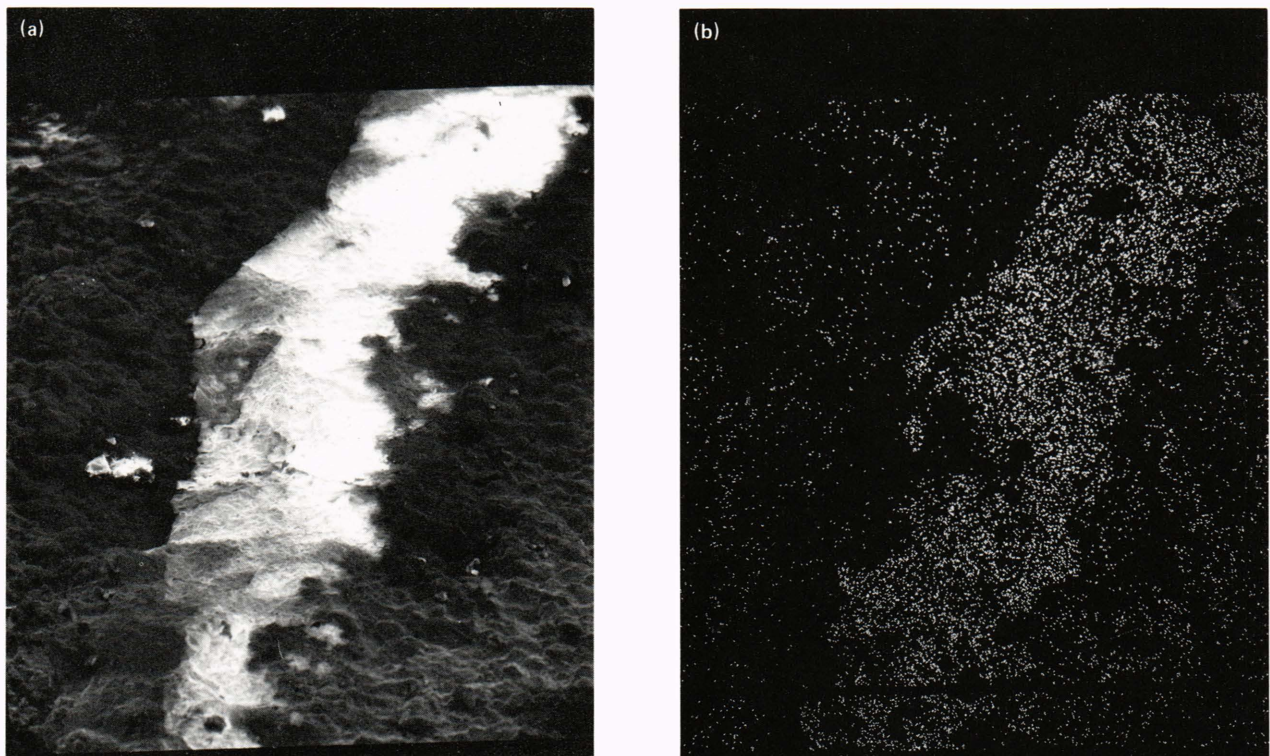

Figure 20—Thoriated tungsten nozzle insert after test firing, magnification 100x. (a) Scanning electron microscope photograph; (b) thorium map.

Specimen-Current Image of a Single Crystal at Low Beam Energies," *Phys. Rev. Lett.* **48**, 882-885 (1982).

[2] C. B. Bargeron, B. H. Nall, and A. N. Jette, "Oxygen Adsorption on the Aluminum (111) Surface by Low-Energy Current Image Diffraction: A New Approach," *Surf. Sci.* **120**, L483-L486 (1982).

[3] A. N. Jette, B. H. Nall, and C. B. Bargeron, "Low Energy Electron Channeling Observed by Current Image Diffraction (CID)," *J. Vac. Sci. Technol.* **A2**, 978-982 (1984).

[4] R. E. Dietz, E. G. McRae, and R. L. Campbell, "Saturation of the Image Potential Observed in Low-Energy Electron Reflection at Cu(001) Surface," *Phys. Rev. Lett.* **45**, 1280-1284 (1980).

[5] C. B. Bargeron, B. H. Nall, and A. N. Jette, "Low-Energy Electron Current Image Diffraction (CID) of the Basal Plane of Titanium," *Surf. Sci.* **139**, 219-230 (1984).

[6] R. M. Lum and L. G. Feinstein, "Investigation of the Molecular Processes Controlling Corrosion Failure Mechanisms in Plastic Encapsulated Semiconductor Devices," *Microelectron. Reliab.* **21**, 15-31 (1981).

[7] P. W. Schuessler, "Adhesive Die Attach Materials: Their Pros and Cons," *Int. J. Hybrid Microelectron.* **6**, 342-345 (1983).

[8] D. M. Shenfield and M. C. Zyetz, "An Investigation of the Effect of 150°C Storage on the Electrical Resistance of Conductive Adhesive Attachment of 2N2222A Transistors," *Int. J. Hybrid Microelectron.* **6**, 346-351 (1983).

[9] R. J. Gale, "Epoxy Degradation Induced Au-Al Intermetallic Void Formation in Plastic Encapsulated MOS Memories," in *Proc. 1984 International Reliability Physics Symp.*, pp. 37-47 (1984).

[10] H. K. Charles, Jr., B. M. Romenesko, G. D. Wagner, R. C. Benson, and O. M. Uy, "The Influence of Contamination on Aluminum-Gold Intermetallics," in *Proc. 1982 International Reliability Physics Symp.*, p. 126 (1982).

[11] E. S. Dettmer, H. K. Charles, Jr., R. C. Benson, B. H. Nall, F. G. Satkiewicz, C. B. Bargeron, and T. E. Phillips, "Epoxy Characterization and Testing Using Mechanical, Electrical, and Surface Analysis Techniques," *Int. J. Hybrid Microelectron.* **6**, 375-386 (1983).

[12] R. C. Benson, B. H. Nall, F. G. Satkiewicz, and H. K. Charles, Jr., "Surface Analysis of Adsorbed Species from Epoxy Adhesives Used in Microelectronics," *Appl. Surf. Sci.* **21**, 219-229 (1985).

[13] R. W. Vasofsky, A. W. Czanderna, and K. K. Czanderna, "Mass Changes of Adhesives During Curing, Exposure to Water Vapor, Evacuation, and Outgassing, Part I: Ablefilms 529, 535, and 550," *IEEE Trans. Compon., Hybrids Manuf. Tech.* **CHMT-1**, 405-411 (1978).

ACKNOWLEDGMENT—The authors wish to thank all our collaborators from other departments, and in particular H. K. Charles, Jr., B. M. Romenesko, and E. S. Dettmer of the Microelectronics Group; O. M. Uy, A. C. Sadilek, J. E. Heiss, H. G. Fox, and W. Wilkinson of the Space Department; and R. M. Rivello and L. B. Weckesser of the Aeronautics Department.

THE AUTHORS

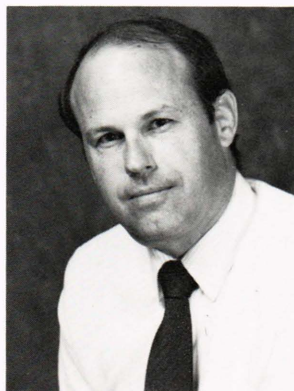

Richard C. Benson (left)

C. Brent Bargeron (center)

A. Norman Jette (right)

RICHARD C. BENSON was born in 1944 and was educated at Michigan State University (B.S. in physical chemistry, 1966) and the University of Illinois (Ph.D. in physical chemistry, 1972). Since joining APL in 1972, he has been a member of the Milton S. Eisenhower Research Center and is manager of the Surface Science Program. He is currently involved in research on the properties of materials used in microelectronics and the application of optical techniques to surface science. Dr. Benson has also conducted research in Raman scattering, optical switching, laser-induced chemistry, chemical lasers, energy transfer, chemiluminescence, fluorescence, and microwave spectroscopy. He is a member of the American Physical Society and the American Vacuum Society.

C. BRENT BARGERON joined APL in 1971 as a member of the Milton S. Eisenhower Research Center. Born in Provo, Utah, in 1943, he earned a Ph.D. degree in physics at the University of Illinois (1971). His thesis was in high-pressure physics. Since joining APL, Dr. Bargeron has been involved in problems in solid-state physics, light scattering, chemical lasers, arterial geometry, corneal damage from infrared radiation, mineral deposits in pathological tissue, quality control and failure analysis of microelectronic components, electron physics, and surface science.

NEWMAN deHAAS's biography and photograph can be found on p. 186.

R. BEN GIVENS's biography and photograph can be found on p. 199.

A. NORMAN JETTE was born in Portland, Ore., in 1934 and received the Ph.D. degree in physics from the University of California, Riverside, in 1965. Before joining APL that year, he was a research associate at the Columbia Radiation Laboratory of Columbia University in New York City. At APL, Dr. Jette has worked in the Milton S. Eisenhower Research Center on theoretical problems in atomic, molecular, and solid-state physics. He provided theoretical support to the program to detect leaks in underground natural gas distribution lines. In 1972 he was visiting professor of physics at the Catholic University of Rio de Janeiro, and in 1980 he was visiting scientist at the Center for Interdisciplinary Research at the University of Bielefeld, West Germany.

Berry H. Nall (left)

Terry E. Phillips (center)

Frank G. Satkiewicz (right)

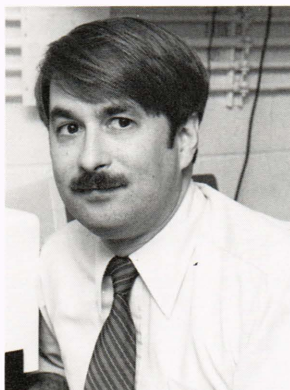

BERRY H. NALL was born near Mobile, Ala., in 1918, and came to APL in the summer of 1948. He obtained an M.S. degree in mechanics (acoustics) from The Catholic University of America in 1970. Mr Nall has been involved with the measurement of the threshold ionization of gases, the acoustic response of burning and non-burning solid propellants, particulate attenuation in acoustic cavities, spurious signals in acoustic surface wave devices, and, more recently, with Auger electron spectroscopy, a technique for surface compositional analysis. He is a member of the Materials Science Group in the Milton S. Eisenhower Research Center.

TERRY E. PHILLIPS is a senior staff chemist in the Materials Science Group in the Milton S. Eisenhower Research Center. Born in Sunbury, Pa., he received a B.A. from Susquehanna University, and M.S. and Ph.D. degrees in chemistry from The Johns Hopkins University in 1976. After completing postgraduate studies at Northwestern University in low-dimensional organic conductors, he joined APL in 1979. He has been involved in problems in photoelectrochemical energy conversion, inorganic optical and electrical phase transition compounds and materials characterization with X rays, nuclear magnetic resonance, mass spectroscopy, and optical spectroscopic techniques.

FRANK G. SATKIEWICZ is a member of the Materials Science Group of the Milton S. Eisenhower Research Center. A native of Cambridge, Mass., he earned degrees in chemistry at Northeastern University (B.S.), Wesleyan University (M.A.), and M.I.T. (Ph.D.).

Prior to his Ph.D studies, he was a radiochemist at Tracerlab, Inc., and a high school teacher. Subsequently, he was employed at Norton Co., doing research on abrasives, refractories, and zeolites. He later worked on the principal staff of GCA Corp. in developing materials for space applications and as a consultant in using sputter-ion source mass spectrometry for studying solids. Since joining APL in 1973, Dr. Satkiewicz has concentrated on using and improving secondary ion mass spectrometry for the analysis of solids and recently has been conducting experiments on the acoustical response of metals when subjected to an ion beam.